

Tuning the hydrogen desorption of $\text{Mg}(\text{BH}_4)_2$ through Zn alloying

D. Harrison and T. Thonhauser*

Department of Physics, Wake Forest University, Winston-Salem, NC 27109, USA.

(Dated: August 4, 2021)

We study the effect of Zn alloying on the hydrogen desorption properties of $\text{Mg}(\text{BH}_4)_2$ using *ab initio* simulations. In particular, we investigate formation/reaction enthalpies/entropies for a number of compounds and reactions at a wide range of temperatures and Zn concentrations in $\text{Mg}_{1-x}\text{Zn}_x(\text{BH}_4)_2$. Our results show that the thermodynamic stability of the resulting material can be significantly lowered through Zn alloying. We find that e.g. the solid solution $\text{Mg}_{2/3}\text{Zn}_{1/3}(\text{BH}_4)_2$ has a reaction enthalpy for the complete hydrogen desorption of only 25.3 kJ/mol H_2 —a lowering of 15 kJ/mol H_2 compared to the pure phase and a corresponding lowering in critical temperature of 123 K. In addition, we find that the enthalpy of mixing is rather small and show that the decrease in reaction enthalpy with Zn concentration is approximately linear.

PACS numbers: 63.20.dk, 65.40.-b, 61.50.Ah

I. INTRODUCTION

Metal borohydrides are amongst the most promising hydrogen storage materials,^{1–5} as they have some of the highest storage densities. Unfortunately, the hydrogen desorption temperature for the most attractive borohydrides is too high for on-board storage, where it should be below 85°C.^{6,7} Thus, borohydrides have been studied intensely in order to lower their desorption temperature. Destabilizing via reactions with other hydrides has been suggested,^{8–11} as well as simple doping,^{12,13} cation substitution,¹⁴ anion substitution,¹⁵ or adding catalysts¹⁶—but unfortunately, the results still fall short of the required DOE targets.⁶

The borohydride $\text{Mg}(\text{BH}_4)_2$ is of particular interest; it has substantial storage density of 14.9 mass% and its decomposition has been shown to be fully reversible under certain conditions,¹⁷ but it completes its first major intermediate step around 570 K and doesn't fully desorb until it reaches temperatures around 820 K.^{11,18} If we can lower its desorption temperature, it might be one of the few materials to satisfy the DOE targets. The desorption temperature is determined by the thermodynamics and kinetics of the desorption reaction. Although it is generally believed that kinetics is the “culprit” in the case of $\text{Mg}(\text{BH}_4)_2$,¹⁹ it is still desirable to first optimize the thermodynamics before addressing the kinetic barrier.¹⁰ In the present manuscript, we investigate the thermodynamics of the desorption of $\text{Mg}(\text{BH}_4)_2$ and the dramatic effect Zn alloying has on it.

We have recently become aware of some very nice work also studying Mg/Zn borohydride solid solutions, and will use this opportunity to compare our results with theirs and point out similarities and differences.²⁰ Further simulations have been performed studying the desorption of $\text{Mg}(\text{BH}_4)_2$,^{21,22} but without accounting for van der Waals contributions, known to be necessary to achieve the correct energetic ordering among polymorphs of $\text{Mg}(\text{BH}_4)_2$;^{23,24} we will thus compare our results of the desorption pathway with other works to ascertain the ef-

fect of van der Waals interactions. We also argue that given the minimum practical delivery pressure from storage system of 3 bar, the overall desorption reaction is, in fact, outside the ideal thermodynamic window of -40°C to $+85^\circ\text{C}$,⁶ but can be brought there by alloying with Zn. We also find a linear relationship between the overall hydrogen desorption enthalpy and Zn concentration in $\text{Mg}(\text{BH}_4)_2$.

Borohydrides are complex hydrides, in which tetrahedral anion units, such as $[\text{BH}_4]^-$ and $[\text{AlH}_4]^-$, are bound to more electropositive cations, such as Li, Na, K, Mg, and Ca. The ionic bonding and charge transfer between the cations and the anion units is a key feature of the stability of these hydrides.²⁵ Targeting this feature, the desorption temperature of Mg_2NiH_4 was successfully lowered by destabilizing it through cation substitution.¹⁴ The same can also be achieved by altering the anion complex, as demonstrated with fluorine substitution in the hydrogen sublattice of Na_3AlH_6 .^{1,15} More generally, an extensive experimental study revealed an almost linear correlation between the desorption temperature T_d in K and the Pauling electronegativity χ_P as well as the hydrogen desorption reaction enthalpy ΔH_r in kJ/mol H_2 :²⁶

$$T_d = 1234 - 517.3 \chi_P, \quad (1)$$

$$T_d = 423.4 + 8.34 \Delta H_r. \quad (2)$$

The study included data for $\mathcal{M}(\text{BH}_4)_n$ with $\mathcal{M} = \text{Li}, \text{Na}, \text{K}, \text{Mg}, \text{Zn}, \text{Sc}, \text{Zr},$ and Hf ,²⁵ and was later extended by Ca, Ti, V, Cr, and Mn.²⁷ $\text{Zn}(\text{BH}_4)_2$ stands out in that it has the lowest temperature for full decomposition of only 410 K.²⁸ $\text{Zn}(\text{BH}_4)_2$ itself is thermodynamically unstable at room temperature and produces diborane gases in its decomposition reaction—it is thus not directly interesting for hydrogen storage. But, as we will argue below, Zn is an ideal alloyant for the $\text{Mg}(\text{BH}_4)_2$ system, forming $\text{Mg}_{1-x}\text{Zn}_x(\text{BH}_4)_2$, with remarkable effects. Zn alloying of $\text{Mg}(\text{BH}_4)_2$ is supported by the following facts: (i) Zn alloying has been found experimentally to significantly lower the decomposition temperature;^{20,29} (ii) Zn alloying lowers the decomposition temperature

of other borohydrides;³⁰ (iii) Zn is known to form a borohydride with the same stoichiometry as $\text{Mg}(\text{BH}_4)_2$ and their structures are essentially the same²⁵ (the ionic radii of Zn and Mg of 0.88 and 0.86 Å are virtually identical); (iv) alloying in other borohydrides, such as $\text{Li}_{1-x}\text{Cu}_x\text{BH}_4$, shows a desorption temperature between the two constituents;^{12,31} (v) Zn is known to not form hydrides or borides like other borohydrides,²⁵ simplifying the hydrogen desorption reaction significantly; and finally (vi) Zn is an abundant major industrial metal.

II. COMPUTATIONAL DETAILS

In order to study the thermodynamics of $\text{Mg}(\text{BH}_4)_2$ and the effect of Zn alloying, we need the enthalpies and entropies for all materials suspected in the decomposition of $\text{Mg}(\text{BH}_4)_2$. To this end, we performed *ab initio* simulations at the DFT level, as implemented in VASP,^{32,33} to calculate the ground-state energies and phonon densities of states. We used PAW pseudopotentials with a 650 eV kinetic energy cutoff and an energy convergence criterion of 10^{-7} eV. We used k -point meshes giving convergence to within 1 meV/atom, with the exception of the metallic compounds and elemental boron, which were converged to within 3 meV/atom. This yielded a k -point mesh of e.g. $5 \times 5 \times 4$ for small unit cells like MgB_2 and a mesh of $1 \times 1 \times 1$ for large unit cells like $\text{Mg}(\text{BH}_4)_2$. Structures were relaxed with respect to unit-cell parameters and atom positions until all forces were less than 0.1 meV/Å. This way, we found the lowest-energy structure of boron to be the 106 atom β -rhombohedral structure suggested by van Setten et al.³⁴ Phonons were calculated with the symmetry-reduced finite-displacement method with displacements of 0.015 Å. Supercells were created such that they were the same dimensions as the k -point mesh used for the original unit cell. The exceptions were the metals Mg and Zn, whose phonons were calculated with a $5 \times 5 \times 2$ supercell and a $3 \times 3 \times 4$ k -point mesh.

While the ground-state structure of $\text{Mg}(\text{BH}_4)_2$ is experimentally known to be of $P6_122$ symmetry with 30 formula units per unit cell, theoretical studies with a variety of exchange-correlation (XC) functionals find numerous other structures, all disagreeing with experiment.²⁴ The reason for this is that $\text{Mg}(\text{BH}_4)_2$ —similar to other borohydrides³⁵—exhibits a small but important contribution from van der Waals interactions, on the order of 0.1 eV per BH_4 unit. Including those contributions via the XC functional vdW-DF^{36,37}—with the (semi)local XC as originally defined in Ref. [38]—we were the first to find the correct ground-state structure in agreement with experiment.²⁴ We further found that the closely related $P3_112$ structure is less than 1 meV per atom higher in energy. This structure has only 9 formula units per unit cell and the local coordination is almost identical to the $P6_122$ structure, resulting in almost identical phonon densities of states. Thus, in the present study we are using vdW-DF and the numerically feasible $P3_112$ struc-

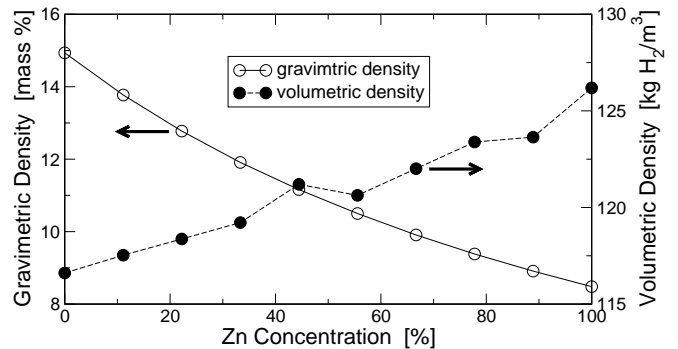


FIG. 1. H_2 gravimetric storage density in mass% (to be read off the left axis) and H_2 volumetric storage density in $\text{kg H}_2/\text{m}^3$ (right axis) for different Zn concentrations.

ture for all our simulations. This is further justified by comparing one of our reaction enthalpies to the results of Albanese et al. in Ref. [20], who in fact used the large $P6_122$ structure and obtained almost identical results—see details below. As our structure has 9 formula units per unit cell, we report results for Zn concentrations in steps of 1/9. Alloying was done by randomly replacing Mg atoms with Zn, with variations—due to which atoms are being replaced—being on the order of only fractions of a kJ/mol at the most. Our results for the enthalpy of mixing compare well with Albanese et al., who found similarly small values.²⁰

III. RESULTS

A. Storage Densities

The gravimetric storage density of $\text{Mg}(\text{BH}_4)_2$ will decrease with increasing Zn content, as can be seen in Fig. 1. But, as we shall see below, only modest alloying is necessary to achieve the required effect, and the loss in gravimetric density is reasonable. On the other hand, the volumetric density increases with increasing Zn content. The “bump” or deviation from linear behavior, observed in Fig. 1 around 50% Zn concentration, is also seen in the work of Albanese et al.,²⁰ and may be indicative of the formation of a superstructure.

B. Structural Stability and Ionic Character

We begin by analyzing the structural stability in terms of the ionic character as a function of Zn concentration. As mentioned above, the ionic bonding is a key feature of the stability of borohydrides. In Table I we quantify this picture and present a Bader charge analysis as a function of Zn concentration, using the fast implementation proposed by Henkelman et al.³⁹ Note that the Bader analysis, similarly to the Mulliken analysis, is an intuitive (but not unique) way of partitioning the electron charge.

TABLE I. Bader charges (in units of e) for the metal site \mathcal{M} and the BH_4 units as a function of concentration x in $\text{Mg}_{1-x}\text{Zn}_x(\text{BH}_4)_2$. Given are also the Pauling electronegativity χ_P and the estimated desorption temperature T_d (in K) from Eq. (1). The reported charges and electronegativities are values averaged over all 9 formula units in the unit cell.

| x | 0 | 1/9 | 2/9 | 3/9 | 4/9 | 5/9 | 6/9 | 7/9 | 8/9 | 1 |
|---------------|-------|-------|-------|-------|-------|-------|-------|-------|-------|-------|
| \mathcal{M} | +1.72 | +1.65 | +1.59 | +1.53 | +1.46 | +1.40 | +1.33 | +1.26 | +1.20 | +1.13 |
| BH_4 | -0.86 | -0.83 | -0.79 | -0.76 | -0.73 | -0.70 | -0.67 | -0.63 | -0.60 | -0.56 |
| χ_P | 1.20 | 1.24 | 1.29 | 1.33 | 1.38 | 1.42 | 1.47 | 1.51 | 1.56 | 1.60 |
| T_d | 613 | 593 | 567 | 546 | 520 | 499 | 474 | 453 | 427 | 406 |

Interestingly, even for the pure $\text{Mg}(\text{BH}_4)_2$ structure, the ionic character significantly deviates from the nominal values of +2 and -1. As expected, the ionic character diminishes as a function of Zn concentration due to the higher electronegativity of Zn, approximately 0.06 e per 10% Zn. A more detailed analysis of the charge density reveals the following: While the direct effect of Zn is localized, hydrogens further away from Zn get a small compensating charge if they are within a tetrahedra next to a Zn. Through this mechanism, even low levels of alloying influence almost the entire structure. In Table I we also show the Pauling electronegativity χ_P as a function of Zn concentration and the corresponding estimated desorption temperatures T_d according to Eq. (1). Purely based on this experimentally found connection for borohydrides, we can already estimate that modest Zn alloying might reduce the desorption temperature on the order of 100 K. In the remainder of this paper, we will quantify this empirical estimate.

C. Thermodynamics of the Hydrogen Desorption at 1 Bar Hydrogen Pressure

We now move to the main point of this paper, i.e. the thermodynamics of the hydrogen desorption and the effect of Zn alloying. To this end, we calculate the temperature dependent vibrational contribution to the enthalpy and entropy as

$$H_{\text{vib}} = \int_0^\infty d\omega \left(\frac{1}{2} + \frac{1}{\exp[\hbar\omega/kT] - 1} \right) g(\omega) \hbar\omega, \quad (3)$$

$$S_{\text{vib}} = \int_0^\infty d\omega \left(\frac{\hbar\omega}{2T} \coth \frac{\hbar\omega}{2kT} - k \ln \left[2 \sinh \frac{\hbar\omega}{2kT} \right] \right) g(\omega), \quad (4)$$

where ω is the vibrational frequency, $g(\omega)$ is the phonon density of states, T is the temperature, and k is Boltzmann's constant. The enthalpy then is the sum of the DFT ground-state energy and this vibrational contribution. Formation enthalpies, in turn, are calculated as differences in enthalpies of the material and its constituent elements (thus, elements in their natural state have formation enthalpies of 0). From this, we calculate enthalpies and entropies of reaction, using formation enthalpies and absolute entropies of all materials (tabulated in the appendix). For reactions involving Zn alloying (Reactions 2, 3, and 13 in Table II), the entropy of

mixing was calculated according to

$$S_{\text{mix}} = -k_B [c \ln c + (1 - c) \ln (1 - c)], \quad (5)$$

where c is the concentration of Zn; this entropy of mixing was added to the entropy of reaction calculated from vibrational frequencies, resulting in e.g. a decrease in reaction entropy of ~ 5 J/K/mol H_2 and a corresponding increase in the critical temperature of ~ 10 K. Note that all structures we found are true local minima and none of the density of states show imaginary frequencies.

Following the approach of van Setten et al.,²² the temperature-dependent thermodynamic values of H_2 were obtained using experimental data.⁴⁰ In particular, we used $H_{\text{H}_2 \text{ gas}}(T) = E_{\text{H}_2} + E_{\text{H}_2}^{\text{ZPE}} + H_{\text{H}_2 \text{ gas}}^{\text{exp}}(T)$, where the electronic energy E_{H_2} and zero-point energy $E_{\text{H}_2}^{\text{ZPE}}$ were calculated using DFT and the last term was taken from experiment.⁴⁰ Specifically, data was taken from H_2 at 1 bar for increments of 100 K with values in between being linearly interpolated. Note that the enthalpy of H_2 changes very little over moderate pressure changes (e.g. the change in enthalpy going from 1 to 100 bar at 300 K is only 0.114 kJ/mol), meaning our formation enthalpies should be useful even when looking at high pressures. The entropy of hydrogen gas used to calculate the entropies of reaction in Table II and the reactions at 3 bar discussed later on were likewise taken from the same experimental data.⁴⁰ For reference, the entropies of H_2 at 300 K for 1 and 3 bar are 130.77 and 121.63 J/K/mol H_2 , respectively. Note that the entropy of hydrogen gas for other pressures can be accurately estimated by the equation $S_{\text{H}_2} = -R \ln p + S_0$, where p is the pressure in bar and S_0 is the entropy at 1 bar.

The overall energy required for the hydrogen decomposition reaction to start can be split into two pieces, i.e. the *reaction enthalpy* and an additional *kinetic barrier*. We argue that the latter is similar for the initial hydrogen release of many decomposition reactions of borohydrides and focus first on the reaction enthalpies. Table II contains the most pertinent results from this study; it lists reaction enthalpies for a number of possible reactions, calculated from formation enthalpies for a range of materials. Where a direct comparison with experiment is possible, we generally find very good agreement. For example, experimental formation enthalpies for MgH_2 and MgB_2 of -75.3 and -41.2 kJ/mol are in excellent agreement with our calculated values of -78.7 and -43.4 kJ/mol (see appendix A).^{42,43} Furthermore,

TABLE II. Reaction enthalpies ΔH_r in kJ/mol H_2 and entropies ΔS_r in J/K/mol H_2 at 300 K for several $Mg(BH_4)_2$ desorption reactions. The critical temperature T_c predicted from the van't Hoff equation $\ln p = -\Delta H/RT + \Delta S/R$ for 1 bar H_2 pressure is given in K. We give a rough estimate of the kinetic barrier in K as the difference $T_{\text{barrier}} = T_d - T_c$, where T_d is the approximate experimental desorption temperature.

| No. | Reactants | → | Products | ΔH_r^{300K} | ΔS_r^{300K} | T_c | T_d | T_{barrier} |
|-----|--|---|--|---------------------|---------------------|-------|------------------|----------------------|
| 1 | $Mg(BH_4)_2$ | → | $MgB_2 + 4H_2$ | 40.3 | 112.15 | 360 | 820 ^a | 460 |
| 2 | $Mg_{2/3}Zn_{1/3}(BH_4)_2$ | → | $\frac{2}{3}MgB_2 + \frac{1}{3}Zn + \frac{2}{3}B + 4H_2$ | 25.3 | 106.72 | 237 | | |
| 3 | $Mg_{1/3}Zn_{2/3}(BH_4)_2$ | → | $\frac{1}{3}MgB_2 + \frac{2}{3}Zn + \frac{1}{3}B + 4H_2$ | 10.4 | 106.57 | 98 | | |
| 4 | $Zn(BH_4)_2$ | → | $Zn + 2B + 4H_2$ | -3.92 | 112.57 | -35 | 410 ^b | 445 |
| 5 | $Mg(BH_4)_2$ | → | $\frac{1}{6}MgB_{12}H_{12} + \frac{5}{6}MgH_2 + \frac{13}{6}H_2$ | 24.8 | 104.71 | 237 | 570 ^c | 333 |
| 6 | MgH_2 | → | $Mg + H_2$ | 78.7 | 132.99 | 592 | 640 ^d | 48 |
| 7 | $\frac{1}{6}MgB_{12}H_{12}$ | → | $\frac{1}{6}Mg + 2B + H_2$ | 85.4 | 119.30 | 716 | 730 ^d | 14 |
| 8 | $Mg(BH_4)_2$ | → | $\frac{1}{6}MgB_{12}H_{12} + \frac{5}{6}Mg + 3H_2$ | 39.8 | 112.56 | 353 | | |
| 9 | $\frac{1}{6}MgB_{12}H_{12} + \frac{5}{6}Mg$ | → | $MgB_2 + H_2$ | 42.0 | 110.91 | 379 | | |
| 10 | $\frac{1}{6}MgB_{12}H_{12}$ | → | $\frac{1}{6}MgH_2 + 2B + \frac{5}{6}H_2$ | 86.8 | 116.56 | 744 | | |
| 11 | $\frac{1}{6}MgB_{12}H_{12} + \frac{5}{6}MgH_2$ | → | $\frac{1}{2}MgB_4 + \frac{1}{2}MgH_2 + \frac{4}{3}H_2$ | 63.5 | 121.13 | 525 | | |
| 12 | $Mg(BH_4)_2$ | → | $MgH_2 + 2B + 3H_2$ | 42.0 | 108.00 | 389 | | |
| 13 | $Mg_{4/5}Zn_{1/5}(BH_4)_2$ | → | $\frac{4}{5}MgH_2 + \frac{1}{5}Zn + 2B + \frac{16}{5}H_2$ | 30.5 | 104.98 | 291 | | |

^aRef. [18]; ^bRef. [28]; ^cRef. [41]; ^dRef. [11].

our calculated reaction enthalpies for Reactions 1 and 8 of 40.3 kJ/mol H_2 and 39.8 kJ/mol H_2 are also in good agreement with the value of 40 ± 2 kJ/mol H_2 found by Yan et al. in Ref. [41].⁴⁴ Previous theoretical studies have calculated an overall reaction enthalpy of 38–39 kJ/mol H_2 at room temperature,^{19,21,22,45} which closely agrees with our value of 40.3 kJ/mol H_2 . We attribute the difference to vdW-DF, which stabilizes $Mg(BH_4)_2$ with respect to its reaction products by accounting for the long-range van der Waals forces. Comparison of our results for other decomposition reactions with previous studies shows similar agreement, with differences on the order of several kJ/mol H_2 due to vdW-DF. Although accounting for long-range van der Waals forces has been found to be critical to finding the correct energetic ordering among polymorphs in borohydrides,^{23,24} it seems to affect total reaction enthalpies by only several kJ/mol H_2 at the most.

Reactions 1 – 4 of Table II show the effects of Zn alloying on the overall reaction enthalpy. We find the effect to be linear and every 10% Zn results in a further lowering of the desorption enthalpy by approximately 4.5 kJ/mol H_2 , as can be seen in Fig. 2. Zn alloying thus provides a convenient way of tuning the desorption enthalpy over a wide range. Note that the desorption enthalpy of Reactions 2 and 5 are approximately the same, but the important difference is that the alloyed phase releases the entire hydrogen, while the latter only releases half of the available hydrogen. Furthermore, note that Reactions 1 – 4 are different from the decomposition modeled in Ref. [20] in that we model the entire hydrogen release, i.e. the outcome is $MgB_2 + 4H_2$, whereas they assume the intermediate MgH_2 . For comparison, we have modeled their reaction also (Reaction 13 in Table II), obtaining 30.5 kJ/mol H_2 in excellent agreement to their value of 30 kJ/mol H_2 —in fact, justifying approximations that both our groups have made. It is important

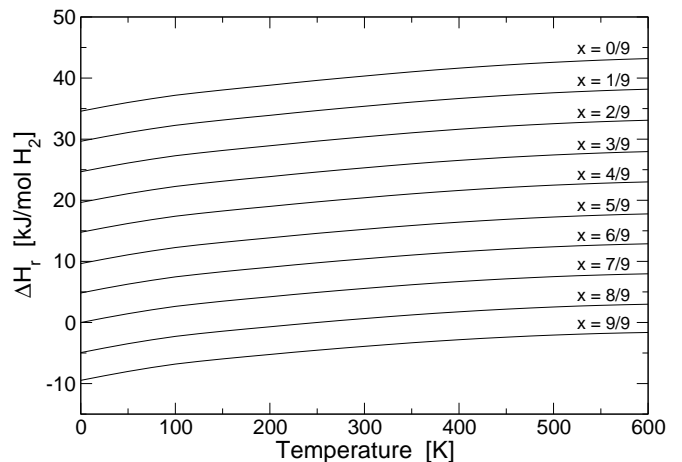


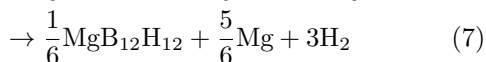
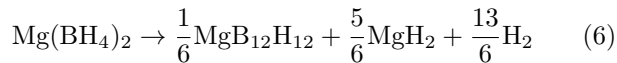
FIG. 2. Reactions enthalpies ΔH_r can readily be calculated from the tabulated data in the appendices. As an example, we plot here the reaction enthalpy as a function of temperature and alloying for the reaction $Mg_{1-x}B_2(1-x) + Zn_x + 2B_x + 4H_2$. Note that the effect of Zn concentration on the reaction enthalpy is almost perfectly linear.

to also compare the two corresponding “pure” reactions, i.e. Reaction 1 and 12. The reaction enthalpy for the entire hydrogen release in Reaction 1 is, in fact, a little lower compared to Reaction 12, which led us to pursue the pure reaction pathway.

Note that we did not list the effects of Zn alloying on intermediate reactions because it was unknown whether Zn would remain in $MgB_{12}H_{12}$ or phase separate, and in either case there was no experimental data on the corresponding structures. Reactions 5 – 7 show suspected intermediate steps, while Reactions 8 – 13 show alternative reactions discussed later; data for other possible

reactions can be readily calculated using extensive thermodynamic data tabulated in the appendix.

Of course, it is also well known that there are more intermediates in the decomposition of $\text{Mg}(\text{BH}_4)_2$ involving $\text{Mg}(\text{B}_x\text{H}_y)_z$ complexes,^{19,46} especially in the formation and decomposition of $\text{MgB}_{12}\text{H}_{12}$. While we did not study all of these possible intermediates, our calculated thermodynamic values in the appendix can give insight into some other favorable pathways. Within the framework of pathways considered, our results show that the most favorable pathway for hydrogen desorption that agrees with experiment is:



Thermodynamically, as seen in Reaction 9, the most favorable pathway after the formation of $\text{MgB}_{12}\text{H}_{12}$ is the formation of MgB_2 , but from experimental differential scanning calorimetry and chemical intuition, it is likely that there is at least one intermediate step from $\text{MgB}_{12}\text{H}_{12}$ to MgB_2 . The theoretical total hydrogen loss for steps (6), (7), and (9) is 8.1%, 11.2%, and 14.9%, respectively. The formation of $\text{MgB}_{12}\text{H}_{12}$, MgH_2 , Mg , and MgB_2 are all well-known steps confirmed by X-ray diffraction and solid state NMR.^{11,18,47,48} They are also supported as thermodynamically favorable by a number of theoretical studies.^{21,49} Furthermore, the temperature evolution of the reaction products also supports this reaction pathway: MgH_2 appears first, then Mg without MgH_2 , and finally MgB_2 .

Equation (6) also corresponds to the mass% of hydrogen desorbed for certain temperatures held for long periods of time. Yan et al. found that just over 8 mass% of H_2 desorb after 1000 min at 573 K; this corresponds almost exactly to the expected value of 8.1% for Eq. (6).⁴⁷ It is also worth noting that it took over an hour before even 4 mass% of H_2 was desorbed, and the curves for lower temperatures never equilibrated after 1000 min. Due to the sluggish kinetics of this step of the reaction it is difficult to see the individual reaction steps in a typical thermogravimetry curve; by the time only a fraction of $\text{Mg}(\text{BH}_4)_2$ has undergone the first step of the reaction, the temperature has increased so that the second step of the reaction has already begun. However, we can see further evidence for the proposed reaction pathway by the results of Matsunaga et al., who found that $\text{Mg}(\text{BH}_4)_2$ could be rehydrogenated from 11% to 8% at 623 K, which corresponds to the rehydrogenation of Mg to MgH_2 (see Fig. 6 of Ref. [50]).

We also find that the previously suggested decomposition of $\text{MgB}_{12}\text{H}_{12}$ to MgH_2 and elements shown in Reaction 10 to be unfavorable as a second step of the reaction, with a critical temperature of 744 K, and suggest the decomposition of MgH_2 ($T_c = 592$ K) as occurring before

$\text{MgB}_{12}\text{H}_{12}$. After MgH_2 decomposes, we suggest the decomposition of $\text{MgB}_{12}\text{H}_{12}$ as our critical temperature of 716 K coincides closely with the final large dip observed in differential scanning calorimetry plots near 1 bar H_2 pressure.⁴¹ Finally, we find the formation of MgB_4 to be plausible, as evidenced by the favorable thermodynamics of Reaction 11.

Reaction 13 is the decomposition reaction modeled by Albanese et al. as having the optimal decomposition enthalpy;²⁰ our calculated value of 30.5 kJ/mol H_2 is in exact agreement with their result of 30 kJ/mol H_2 . Note that our enthalpy and entropy used for 20% Zn-alloyed $\text{Mg}(\text{BH}_4)_2$ were calculated from a linear interpolation of our thermodynamic data; this is valid because the change in enthalpy and entropy values with Zn concentration is nearly exactly linear (see the appendix). It is interesting to see that, when we interpolate our results for Reactions 1 – 4 to a Zn concentration of 1/5 to match the concentration in Reaction 13, we find a reaction enthalpy and entropy of 31.46 kJ/mol H_2 and 112 J/K/mol H_2 , leading to a critical temperature $T_c = 281$ K, which is essentially the same as for Reaction 13 in Table II. Although our results for Reaction 13 agree with the work done by Albanese et al., our work can be seen as an extension of the theoretical part of that study, as we have actually calculated the full thermodynamic data—including reaction entropies—instead of interpolating them. We have done so for their proposed partial decomposition (Reaction 13) and in addition for a large number of other reactions (Reactions 1 – 11), including the full hydrogen decomposition as well as others that can easily be deduced from the tabulated thermodynamic data in our appendix.

D. Thermodynamics of the Hydrogen Desorption at 3 Bar Hydrogen Pressure

From the results above it follows that kinetics is not the only problem with $\text{Mg}(\text{BH}_4)_2$, as the reaction from $\text{Mg}(\text{BH}_4)_2$ to MgB_2 has a calculated critical temperature of 360 K (86°C). Note that this critical temperature was calculated at 1 bar H_2 pressure, while the minimum DOE target for delivery pressure is around 3 bar; the critical temperature at 3 bar is 430 K (157°C), well outside the optimal thermodynamic window. Furthermore, while Zuttel et al. have argued that the entropic contribution to metal hydride reactions is approximately 130 J/K/mol H_2 for most simple metal-hydrogen systems,⁵¹ lower values can occur for complex metal hydrides, such as 97 J/K/mol H_2 for $\text{LiBH}_4 \rightarrow \text{LiH} + \text{B} + 3/2\text{H}_2$.⁹ It seems likely then that $\text{Mg}(\text{BH}_4)_2$ also has a lower than normal entropy of reaction, in agreement with our calculated values in Table II, given its similarity to LiBH_4 . Because of this comparatively low value for the reaction entropy, even the commonly cited value of 40 kJ/mol H_2 is too high for a practical PEM fuel cell. In fact, using our calculated entropy

value, for a minimum delivery pressure of 3 bar and temperature of 80°C, the maximum desired enthalpy is 33 kJ/mol H₂. Also note that while the estimated desired reaction enthalpy for a hydrogen storage material is 20–50 kJ/mol H₂ (for reactions with low to high entropic contributions), the ideal range for efficiency is 20–30 kJ/mol H₂.⁷ All of this points towards the conclusion that Mg(BH₄)₂ needs to be destabilized with respect to its reaction products in order to achieve the ideal thermodynamic reaction window. E.g. in the case of 1/3 Zn alloying, we find a reaction enthalpy of 25.3 kJ/mol H₂ and a critical temperature of 270 K (−3°C) at 3 bar, both in the ideal range for a PEM fuel cell. This is based on the suspected decomposition reaction $\text{Mg}_{1-x}\text{Zn}_x(\text{BH}_4)_2 \rightarrow \text{Mg}_{1-x}\text{B}_{2(1-x)} + \text{Zn}_x + 2\text{B}_x + 4\text{H}_2$. We find this to be the most likely reaction as Zn(BH₄)₂ “decomposes directly to elemental Zn due to instabilities of Zn hydride and boride,”²⁵ and we find Zn-alloyed MgB₂ to be unstable and expect it to phase separate to MgB₂, Zn, and B based on preliminary calculations. Of course, for high concentrations of Zn, we expect the formation of diborane, as seen experimentally by Albanese et al. and Kalantzopoulos et al.,^{20,29} but for low concentrations of Zn it is known that diborane is not formed.

E. Kinetics of the Hydrogen Desorption and overall Desorption Temperature

We now switch to a discussion of the kinetic barrier. By comparing our calculated critical temperatures T_c with the known experimental temperatures of hydrogen desorption T_d ,^{11,18,28,47} we can make a rough estimate of the kinetic barrier, given in Table II. Interestingly, from Eq. (2) we see that—by definition—borohydrides with $\Delta H_r = 0$ have a kinetic barrier of 423.4 K; using the same argument but a slightly different fit (see footnote 26), we find a kinetic barrier of 439.4 K. Borohydrides with $\Delta H_r \approx 0$, such as Zn(BH₄)₂, thus must have a kinetic barrier of the same order of magnitude, in very good agreement to our calculated value of 445 K for Zn.

From Table II we see that the kinetic barrier for the full hydrogen release reaction is almost the same for Mg(BH₄)₂ and Zn(BH₄)₂, which in turn means that differences in calculated critical temperatures in Table II approximately result in the same differences for the overall desorption temperature. We thus estimate a decrease of desorption temperature of Mg(BH₄)₂ when alloying with Zn for Reaction 1 of approximately 123 K for 1/3 Zn concentration and 262 K for 2/3 Zn. Note that we obtain almost identical numbers using a different argument: Simply evaluating the experimental relationship in Eq. (2), purely based on our calculated changes in enthalpy, gives a lowering of the desorption temperature of

125 K for 1/3 Zn concentration and 250 K for 2/3 Zn.

From our results we see that the formation of the intermediate MgB₁₂H₁₂ is mainly responsible for the kinetic barrier, and methods to improve the kinetics of borohydrides should focus on reaction pathways avoiding the formation of this intermediate, as suggested by several other groups.^{17,18,47} Because the kinetic barrier is roughly constant, at least for the full hydrogen release reaction, we do not expect alloying to have a direct impact on the height of the kinetic barrier. But, it is really the overall energy required to start the hydrogen desorption that is of interest—and that linearly decreases with Zn concentration. Note that the reaction kinetics can, at least in principle, be accelerated by using catalysts or by controlling the particle size of reactants.⁹ Furthermore, it is also conceivable that the kinetics of the dehydrogenation reaction can be influenced by the inclusion of impurities, as studied by van de Walle’s group.¹³

IV. CONCLUSIONS

In summary, *ab initio* calculations were performed to accurately determine formation enthalpies for many different materials suspected in the decomposition of Mg(BH₄)₂, to find reaction enthalpies for the most likely reaction pathways, and to study the effect of Zn concentration on the overall desorption reaction. We find that the overall thermodynamics of the desorption reaction can be optimized by alloying Mg(BH₄)₂ with around 33% Zn. We estimate that in this case the temperature for the complete decomposition reaction is lowered by 123 K. Verifying the kinetics explicitly through *ab initio* calculations is difficult and is the subject of ongoing research. Supported by encouraging experimental results,^{20,29} we conclude that alloying Mg(BH₄)₂ with Zn is an ideal option for fine-tuning the desorption reaction without sacrificing too much gravimetric storage density.

ACKNOWLEDGMENTS

This work was supported in full by NSF Grant No. DMR-1145968.

Appendix A: Standard enthalpies of formation

We give here standard enthalpies of formations for all structures used throughout the main manuscript, calculated from DFT ground-state energies with temperature and zero-point contributions included through Eq. (3). Units of temperature T and enthalpy ΔH are given in K and kJ/mol, respectively. We used experimental data for the temperature contributed enthalpy of H₂ gas.⁴⁰

1. MgB₂

| T [K] | ΔH [kJ/mol] | T [K] | ΔH [kJ/mol] | T [K] | ΔH [kJ/mol] | T [K] | ΔH [kJ/mol] |
|---------|---------------------|---------|---------------------|---------|---------------------|---------|---------------------|
| 25 | -42.8478 | 225 | -43.5773 | 425 | -43.0847 | 625 | -42.5631 |
| 50 | -42.9136 | 250 | -43.5474 | 450 | -43.0123 | 650 | -42.5079 |
| 75 | -43.0676 | 275 | -43.5007 | 475 | -42.9416 | 675 | -42.4547 |
| 100 | -43.2423 | 300 | -43.4422 | 500 | -42.8729 | 700 | -42.4035 |
| 125 | -43.3909 | 325 | -43.3760 | 525 | -42.8063 | 725 | -42.3542 |
| 150 | -43.4969 | 350 | -43.3053 | 550 | -42.7421 | 750 | -42.3067 |
| 175 | -43.5594 | 375 | -43.2321 | 575 | -42.6802 | 775 | -42.2608 |
| 200 | -43.5837 | 400 | -43.1582 | 600 | -42.6205 | 800 | -42.2166 |

$$\Delta H(T = 0) = -42.8445 \text{ kJ/mol}$$

$$\Delta H(E \text{ only}) = -41.3923 \text{ kJ/mol}$$

2. MgH₂

| T [K] | ΔH [kJ/mol] | T [K] | ΔH [kJ/mol] | T [K] | ΔH [kJ/mol] | T [K] | ΔH [kJ/mol] |
|---------|---------------------|---------|---------------------|---------|---------------------|---------|---------------------|
| 25 | -71.2620 | 225 | -77.1642 | 425 | -80.2792 | 625 | -80.6338 |
| 50 | -72.0536 | 250 | -77.7319 | 450 | -80.4525 | 650 | -80.5411 |
| 75 | -72.8916 | 275 | -78.2442 | 475 | -80.5836 | 675 | -80.4248 |
| 100 | -73.7396 | 300 | -78.7003 | 500 | -80.6754 | 700 | -80.2867 |
| 125 | -74.4942 | 325 | -79.1201 | 525 | -80.7307 | 725 | -80.1277 |
| 150 | -75.2186 | 350 | -79.4855 | 550 | -80.7519 | 750 | -79.9499 |
| 175 | -75.9036 | 375 | -79.7983 | 575 | -80.7413 | 775 | -79.7546 |
| 200 | -76.5428 | 400 | -80.0609 | 600 | -80.7012 | 800 | -79.5430 |

$$\Delta H(T = 0) = -70.5096 \text{ kJ/mol}$$

$$\Delta H(E \text{ only}) = -80.7888 \text{ kJ/mol}$$

3. MgB₁₂H₁₂

| T [K] | ΔH [kJ/mol] | T [K] | ΔH [kJ/mol] | T [K] | ΔH [kJ/mol] | T [K] | ΔH [kJ/mol] |
|---------|---------------------|---------|---------------------|---------|---------------------|---------|---------------------|
| 25 | -474.2918 | 225 | -503.3760 | 425 | -523.9349 | 625 | -532.7084 |
| 50 | -478.3169 | 250 | -506.6553 | 450 | -525.6071 | 650 | -533.1555 |
| 75 | -482.1853 | 275 | -509.7199 | 475 | -527.0971 | 675 | -533.4792 |
| 100 | -486.0506 | 300 | -512.5552 | 500 | -528.4145 | 700 | -533.6845 |
| 125 | -489.5086 | 325 | -515.2722 | 525 | -529.5698 | 725 | -533.7732 |
| 150 | -493.0109 | 350 | -517.7585 | 550 | -530.5696 | 750 | -533.7528 |
| 175 | -496.5009 | 375 | -520.0212 | 575 | -531.4215 | 775 | -533.6277 |
| 200 | -499.9106 | 400 | -522.0699 | 600 | -532.1323 | 800 | -533.4021 |

$$\Delta H(T = 0) = -469.9027 \text{ kJ/mol}$$

$$\Delta H(E \text{ only}) = -612.5082 \text{ kJ/mol}$$

4. MgB₄

| T [K] | ΔH [kJ/mol] | T [K] | ΔH [kJ/mol] | T [K] | ΔH [kJ/mol] | T [K] | ΔH [kJ/mol] |
|---------|---------------------|---------|---------------------|---------|---------------------|---------|---------------------|
| 25 | -53.5246 | 225 | -53.8921 | 425 | -53.8095 | 625 | -53.6442 |
| 50 | -53.5565 | 250 | -53.8964 | 450 | -53.7899 | 650 | -53.6232 |
| 75 | -53.6239 | 275 | -53.8942 | 475 | -53.7698 | 675 | -53.6023 |
| 100 | -53.6993 | 300 | -53.8869 | 500 | -53.7492 | 700 | -53.5815 |
| 125 | -53.7661 | 325 | -53.8758 | 525 | -53.7284 | 725 | -53.5607 |
| 150 | -53.8183 | 350 | -53.8619 | 550 | -53.7074 | 750 | -53.5401 |
| 175 | -53.8554 | 375 | -53.8458 | 575 | -53.6864 | 775 | -53.5196 |
| 200 | -53.8792 | 400 | -53.8282 | 600 | -53.6653 | 800 | -53.4992 |

$$\Delta H(T = 0) = -53.5227 \text{ kJ/mol}$$

$$\Delta H(E \text{ only}) = -53.8811 \text{ kJ/mol}$$

5. Zn-alloyed Mg(BH₄)₂

Values are given for all 10 alloying levels of Mg(BH₄)₂ from 0/9 to 9/9. Units for temperature T and enthalpies ΔH are K and kJ/mol, respectively.

| T | $\Delta H(0/9)$ | $\Delta H(1/9)$ | $\Delta H(2/9)$ | $\Delta H(3/9)$ | $\Delta H(4/9)$ | $\Delta H(5/9)$ | $\Delta H(6/9)$ | $\Delta H(7/9)$ | $\Delta H(8/9)$ | $\Delta H(9/9)$ |
|-------------------|-----------------|-----------------|-----------------|-----------------|-----------------|-----------------|-----------------|-----------------|-----------------|-----------------|
| E_{only} | -261.7976 | -236.4970 | -210.9513 | -185.1490 | -159.9197 | -133.7350 | -108.8261 | -83.6754 | -58.5632 | -34.6722 |
| 0 | -181.1409 | -156.6974 | -131.9971 | -107.1175 | -82.8319 | -57.5765 | -33.5969 | -9.4840 | 14.9718 | 37.8973 |
| 25 | -184.1121 | -159.6661 | -134.9744 | -110.0966 | -85.8174 | -60.5598 | -36.5847 | -12.4716 | 11.9706 | 34.8856 |
| 50 | -186.9262 | -162.4711 | -137.7886 | -112.9080 | -88.6331 | -63.3640 | -39.3886 | -15.2746 | 9.1561 | 32.0606 |
| 75 | -189.5518 | -165.0799 | -140.3934 | -115.4973 | -91.2175 | -65.9289 | -41.9403 | -17.8210 | 6.6122 | 29.5198 |
| 100 | -191.9842 | -167.4923 | -142.7930 | -117.8747 | -93.5821 | -68.2694 | -44.2600 | -20.1315 | 4.3123 | 27.2310 |
| 125 | -193.9260 | -169.4133 | -144.6961 | -119.7533 | -95.4431 | -70.1046 | -46.0719 | -21.9319 | 2.5255 | 25.4591 |
| 150 | -195.7116 | -171.1788 | -146.4412 | -121.4734 | -97.1444 | -71.7801 | -47.7249 | -23.5728 | 0.8988 | 23.8480 |
| 175 | -197.3677 | -172.8158 | -148.0571 | -123.0648 | -98.7177 | -73.3288 | -49.2532 | -25.0893 | -0.6041 | 22.3604 |
| 200 | -198.9169 | -174.3473 | -149.5675 | -124.5518 | -100.1878 | -74.7759 | -50.6822 | -26.5069 | -2.0090 | 20.9701 |
| 225 | -200.5059 | -175.9197 | -151.1194 | -126.0814 | -101.7016 | -76.2683 | -52.1583 | -27.9718 | -3.4620 | 19.5312 |
| 250 | -202.0122 | -177.4102 | -152.5902 | -127.5308 | -103.1361 | -77.6828 | -53.5577 | -29.3599 | -4.8388 | 18.1682 |
| 275 | -203.4391 | -178.8220 | -153.9828 | -128.9030 | -104.4940 | -79.0218 | -54.8824 | -30.6729 | -6.1412 | 16.8799 |
| 300 | -204.7866 | -180.1550 | -155.2971 | -130.1978 | -105.7747 | -80.2844 | -56.1313 | -31.9097 | -7.3677 | 15.6677 |
| 325 | -206.1304 | -181.4847 | -156.6087 | -131.4905 | -107.0534 | -81.5459 | -57.3793 | -33.1450 | -8.5931 | 14.4568 |
| 350 | -207.3915 | -182.7322 | -157.8386 | -132.7021 | -108.2511 | -82.7269 | -58.5470 | -34.2996 | -9.7381 | 13.3268 |
| 375 | -208.5682 | -183.8955 | -158.9848 | -133.8306 | -109.3658 | -83.8256 | -59.6324 | -35.3715 | -10.8005 | 12.2795 |
| 400 | -209.6592 | -184.9734 | -160.0461 | -134.8747 | -110.3961 | -84.8403 | -60.6339 | -36.3591 | -11.7789 | 11.3164 |
| 425 | -210.6765 | -185.9779 | -161.0344 | -135.8465 | -111.3540 | -85.7832 | -61.5637 | -37.2747 | -12.6855 | 10.4253 |
| 450 | -211.6066 | -186.8955 | -161.9364 | -136.7324 | -112.2263 | -86.6409 | -62.4083 | -38.1048 | -13.5068 | 9.6196 |
| 475 | -212.4497 | -187.7263 | -162.7521 | -137.5326 | -113.0128 | -87.4133 | -63.1678 | -38.8497 | -14.2430 | 8.8989 |
| 500 | -213.2061 | -188.4708 | -163.4819 | -138.2475 | -113.7141 | -88.1010 | -63.8425 | -39.5098 | -14.8946 | 8.2629 |
| 525 | -213.8777 | -189.1306 | -164.1276 | -138.8788 | -114.3320 | -88.7056 | -64.4344 | -40.0870 | -15.4635 | 7.7095 |
| 550 | -214.4644 | -189.7059 | -164.6892 | -139.4265 | -114.8665 | -89.2273 | -64.9435 | -40.5814 | -15.9497 | 7.2385 |
| 575 | -214.9676 | -190.1980 | -165.1681 | -139.8920 | -115.3189 | -89.6673 | -65.3711 | -40.9945 | -16.3547 | 6.8486 |
| 600 | -215.3889 | -190.6084 | -165.5658 | -140.2768 | -115.6908 | -90.0273 | -65.7189 | -41.3278 | -16.6801 | 6.5381 |
| 625 | -215.7300 | -190.9390 | -165.8841 | -140.5827 | -115.9840 | -90.3089 | -65.9885 | -41.5831 | -16.9276 | 6.3052 |
| 650 | -215.9928 | -191.1914 | -166.1248 | -140.8114 | -116.2003 | -90.5139 | -66.1818 | -41.7623 | -17.0992 | 6.1480 |
| 675 | -216.1793 | -191.3679 | -166.2899 | -140.9650 | -116.3418 | -90.6445 | -66.3009 | -41.8675 | -17.1969 | 6.0644 |
| 700 | -216.2917 | -191.4705 | -166.3815 | -141.0455 | -116.4104 | -90.7026 | -66.3477 | -41.9007 | -17.2227 | 6.0522 |
| 725 | -216.3300 | -191.4993 | -166.3998 | -141.0531 | -116.4063 | -90.6884 | -66.3225 | -41.8621 | -17.1769 | 6.1115 |
| 750 | -216.2986 | -191.4587 | -166.3489 | -140.9920 | -116.3338 | -90.6061 | -66.2294 | -41.7559 | -17.0636 | 6.2378 |
| 775 | -216.1996 | -191.3507 | -166.2312 | -140.8643 | -116.1951 | -90.4578 | -66.0707 | -41.5843 | -16.8850 | 6.4290 |
| 800 | -216.0355 | -191.1778 | -166.0488 | -140.6724 | -115.9924 | -90.2459 | -65.8486 | -41.3496 | -16.6435 | 6.6828 |

Appendix B: Absolute entropies

Eq. (4). Units for temperature T and entropies S are K and J/K/mol, respectively.

We give here absolute entropies for all structures used throughout the main manuscript, calculated using

1. MgB₂

| T [K] | S [J/K/mol] | T [K] | S [J/K/mol] | T [K] | S [J/K/mol] | T [K] | S [J/K/mol] |
|---------|---------------|---------|---------------|---------|---------------|---------|---------------|
| 25 | 0.0049 | 225 | 23.2048 | 425 | 55.1436 | 625 | 79.7405 |
| 50 | 0.2642 | 250 | 27.5212 | 450 | 58.6030 | 650 | 82.3799 |
| 75 | 1.4697 | 275 | 31.7893 | 475 | 61.9427 | 675 | 84.9384 |
| 100 | 3.7830 | 300 | 35.9743 | 500 | 65.1672 | 700 | 87.4202 |
| 125 | 6.9282 | 325 | 40.0539 | 525 | 68.2817 | 725 | 89.8290 |
| 150 | 10.6248 | 350 | 44.0151 | 550 | 71.2912 | 750 | 92.1687 |
| 175 | 14.6636 | 375 | 47.8514 | 575 | 74.2008 | 775 | 94.4427 |
| 200 | 18.8933 | 400 | 51.5607 | 600 | 77.0157 | 800 | 96.6542 |

2. MgH₂

| T [K] | S [J/K/mol] | T [K] | S [J/K/mol] | T [K] | S [J/K/mol] | T [K] | S [J/K/mol] |
|---------|---------------|---------|---------------|---------|---------------|---------|---------------|
| 25 | 0.0301 | 225 | 21.1051 | 425 | 43.7259 | 625 | 63.4665 |
| 50 | 0.8668 | 250 | 24.0625 | 450 | 46.3667 | 650 | 65.7097 |
| 75 | 2.9991 | 275 | 26.9837 | 475 | 48.9595 | 675 | 67.9047 |
| 100 | 5.8224 | 300 | 29.8698 | 500 | 51.5030 | 700 | 70.0524 |
| 125 | 8.8840 | 325 | 32.7202 | 525 | 53.9965 | 725 | 72.1538 |
| 150 | 11.9888 | 350 | 35.5334 | 550 | 56.4395 | 750 | 74.2101 |
| 175 | 15.0695 | 375 | 38.3071 | 575 | 58.8319 | 775 | 76.2224 |
| 200 | 18.1085 | 400 | 41.0387 | 600 | 61.1741 | 800 | 78.1921 |

3. MgB₁₂H₁₂

| T [K] | S [J/K/mol] | T [K] | S [J/K/mol] | T [K] | S [J/K/mol] | T [K] | S [J/K/mol] |
|---------|---------------|---------|---------------|---------|---------------|---------|---------------|
| 25 | 6.3137 | 225 | 120.6799 | 425 | 270.7316 | 625 | 415.3139 |
| 50 | 20.9873 | 250 | 137.9110 | 450 | 289.7719 | 650 | 431.9936 |
| 75 | 35.4722 | 275 | 155.9381 | 475 | 308.5848 | 675 | 448.3569 |
| 100 | 48.9467 | 300 | 174.5592 | 500 | 327.1345 | 700 | 464.4084 |
| 125 | 61.9336 | 325 | 193.5822 | 525 | 345.3956 | 725 | 480.1542 |
| 150 | 75.1936 | 350 | 212.8384 | 550 | 363.3518 | 750 | 495.6008 |
| 175 | 89.2742 | 375 | 232.1869 | 575 | 380.9930 | 775 | 510.7553 |
| 200 | 104.4286 | 400 | 251.5141 | 600 | 398.3141 | 800 | 525.6249 |

4. MgB₄

| T [K] | S [J/K/mol] | T [K] | S [J/K/mol] | T [K] | S [J/K/mol] | T [K] | S [J/K/mol] |
|---------|---------------|---------|---------------|---------|---------------|---------|---------------|
| 25 | 0.0637 | 225 | 34.4447 | 425 | 80.6957 | 625 | 118.8385 |
| 50 | 1.1818 | 250 | 40.4270 | 450 | 85.9533 | 650 | 123.0205 |
| 75 | 3.8995 | 275 | 46.4271 | 475 | 91.0663 | 675 | 127.0873 |
| 100 | 7.7271 | 300 | 52.3932 | 500 | 96.0356 | 700 | 131.0436 |
| 125 | 12.2816 | 325 | 58.2867 | 525 | 100.8636 | 725 | 134.8940 |
| 150 | 17.3581 | 350 | 64.0798 | 550 | 105.5537 | 750 | 138.6430 |
| 175 | 22.8185 | 375 | 69.7532 | 575 | 110.1098 | 775 | 142.2949 |
| 200 | 28.5473 | 400 | 75.2944 | 600 | 114.5366 | 800 | 145.8538 |

5. Zn-alloyed $\text{Mg}(\text{BH}_4)_2$

Values are given for all 10 alloying levels of $\text{Mg}(\text{BH}_4)_2$ from 0/9 to 9/9. Units for temperature T and entropy S are K and J/K/mol, respectively.

| T | $S(0/9)$ | $S(1/9)$ | $S(2/9)$ | $S(3/9)$ | $S(4/9)$ | $S(5/9)$ | $S(6/9)$ | $S(7/9)$ | $S(8/9)$ | $S(9/9)$ |
|-----|----------|----------|----------|----------|----------|----------|----------|----------|----------|----------|
| 25 | 1.6220 | 2.2841 | 2.2170 | 2.6043 | 2.7088 | 3.3761 | 3.5663 | 4.1165 | 3.6454 | 3.4832 |
| 50 | 8.3785 | 9.8673 | 10.1158 | 11.1473 | 11.7055 | 13.2631 | 14.0306 | 15.1895 | 14.9646 | 15.0737 |
| 75 | 18.0017 | 20.0819 | 20.7124 | 22.3144 | 23.2698 | 25.4639 | 26.7622 | 28.3285 | 28.4614 | 28.9387 |
| 100 | 28.7955 | 31.2783 | 32.2271 | 34.2544 | 35.5285 | 38.1711 | 39.8800 | 41.7232 | 42.1489 | 42.9248 |
| 125 | 39.9059 | 42.6715 | 43.8770 | 46.2207 | 47.7481 | 50.7195 | 52.7340 | 54.7764 | 55.4214 | 56.4269 |
| 150 | 50.9458 | 53.9177 | 55.3307 | 57.9162 | 59.6395 | 62.8582 | 65.0962 | 67.2857 | 68.0931 | 69.2724 |
| 175 | 61.7268 | 64.8542 | 66.4356 | 69.2103 | 71.0836 | 74.4918 | 76.8938 | 79.1943 | 80.1235 | 81.4350 |
| 200 | 72.1649 | 75.4130 | 77.1325 | 80.0582 | 82.0477 | 85.6044 | 88.1291 | 90.5164 | 91.5394 | 92.9545 |
| 225 | 82.2382 | 85.5830 | 87.4171 | 90.4661 | 92.5482 | 96.2238 | 98.8438 | 101.3023 | 102.3994 | 103.8990 |
| 250 | 91.9590 | 95.3833 | 97.3144 | 100.4663 | 102.6246 | 106.3980 | 109.0946 | 111.6142 | 112.7719 | 114.3435 |
| 275 | 101.3544 | 104.8461 | 106.8603 | 110.0999 | 112.3230 | 116.1785 | 118.9395 | 121.5135 | 122.7219 | 124.3569 |
| 300 | 110.4554 | 114.0053 | 116.0920 | 119.4075 | 121.6873 | 125.6133 | 128.4297 | 131.0536 | 132.3055 | 133.9978 |
| 325 | 119.2913 | 122.8923 | 125.0430 | 128.4251 | 130.7555 | 134.7429 | 137.6085 | 140.2788 | 141.5685 | 143.3135 |
| 350 | 127.8875 | 131.5339 | 133.7417 | 137.1828 | 139.5591 | 143.6006 | 146.5106 | 149.2246 | 150.5477 | 152.3417 |
| 375 | 136.2653 | 139.9525 | 142.2114 | 145.7053 | 148.1238 | 152.2135 | 155.1640 | 157.9193 | 159.2723 | 161.1119 |
| 400 | 144.4423 | 148.1666 | 150.4716 | 154.0130 | 156.4703 | 160.6034 | 163.5911 | 166.3856 | 167.7655 | 169.6480 |
| 425 | 152.4333 | 156.1913 | 158.5381 | 162.1224 | 164.6158 | 168.7881 | 171.8103 | 174.6419 | 176.0464 | 177.9691 |
| 450 | 160.2505 | 164.0394 | 166.4242 | 170.0474 | 172.5745 | 176.7823 | 179.8367 | 182.7035 | 184.1304 | 186.0909 |
| 475 | 167.9043 | 171.7216 | 174.1411 | 177.7996 | 180.3582 | 184.5984 | 187.6828 | 190.5831 | 192.0306 | 194.0267 |
| 500 | 175.4037 | 179.2471 | 181.6983 | 185.3892 | 187.9771 | 192.2471 | 195.3595 | 198.2915 | 199.7581 | 201.7877 |
| 525 | 182.7562 | 186.6239 | 189.1041 | 192.8245 | 195.4401 | 199.7373 | 202.8760 | 205.8380 | 207.3223 | 209.3835 |
| 550 | 189.9688 | 193.8589 | 196.3658 | 200.1133 | 202.7547 | 207.0769 | 210.2403 | 213.2308 | 214.7316 | 216.8225 |
| 575 | 197.0471 | 200.9582 | 203.4895 | 207.2619 | 209.9277 | 214.2730 | 217.4595 | 220.4770 | 221.9932 | 224.1120 |
| 600 | 203.9967 | 207.9271 | 210.4811 | 214.2763 | 216.9650 | 221.3316 | 224.5399 | 227.5829 | 229.1135 | 231.2586 |
| 625 | 210.8220 | 214.7706 | 217.3453 | 221.1617 | 223.8719 | 228.2583 | 231.4870 | 234.5542 | 236.0983 | 238.2681 |
| 650 | 217.5274 | 221.4929 | 224.0869 | 227.9228 | 230.6532 | 235.0579 | 238.3058 | 241.3958 | 242.9527 | 245.1457 |
| 675 | 224.1166 | 228.0979 | 230.7098 | 234.5638 | 237.3132 | 241.7350 | 245.0009 | 248.1126 | 249.6814 | 251.8963 |
| 700 | 230.5933 | 234.5894 | 237.2179 | 241.0885 | 243.8558 | 248.2935 | 251.5764 | 254.7085 | 256.2887 | 258.5241 |
| 725 | 236.9606 | 240.9707 | 243.6144 | 247.5006 | 250.2848 | 254.7373 | 258.0361 | 261.1876 | 262.7785 | 265.0332 |
| 750 | 243.2216 | 247.2447 | 249.9027 | 253.8033 | 256.6034 | 261.0697 | 264.3836 | 267.5534 | 269.1543 | 271.4272 |
| 775 | 249.3791 | 253.4144 | 256.0858 | 259.9998 | 262.8148 | 267.2940 | 270.6221 | 273.8092 | 275.4197 | 277.7096 |
| 800 | 255.4358 | 259.4825 | 262.1663 | 266.0928 | 268.9220 | 273.4133 | 276.7547 | 279.9581 | 281.5777 | 283.8837 |

6. Mg

| T [K] | S [J/K/mol] | T [K] | S [J/K/mol] | T [K] | S [J/K/mol] | T [K] | S [J/K/mol] |
|---------|---------------|---------|---------------|---------|---------------|---------|---------------|
| 25 | 0.1591 | 225 | 25.4974 | 425 | 40.3539 | 625 | 49.6940 |
| 50 | 2.0640 | 250 | 27.8794 | 450 | 41.7287 | 650 | 50.6506 |
| 75 | 5.6107 | 275 | 30.0685 | 475 | 43.0327 | 675 | 51.5719 |
| 100 | 9.5667 | 300 | 32.0909 | 500 | 44.2727 | 700 | 52.4604 |
| 125 | 13.3697 | 325 | 33.9685 | 525 | 45.4546 | 725 | 53.3183 |
| 150 | 16.8606 | 350 | 35.7196 | 550 | 46.5835 | 750 | 54.1477 |
| 175 | 20.0248 | 375 | 37.3593 | 575 | 47.6638 | 775 | 54.9504 |
| 200 | 22.8912 | 400 | 38.9005 | 600 | 48.6995 | 800 | 55.7281 |

7. B

| T [K] | S [J/K/mol] | T [K] | S [J/K/mol] | T [K] | S [J/K/mol] | T [K] | S [J/K/mol] |
|---------|---------------|---------|---------------|---------|---------------|---------|---------------|
| 25 | 0.0000 | 225 | 3.3007 | 425 | 11.0926 | 625 | 18.2138 |
| 50 | 0.0061 | 250 | 4.2054 | 450 | 12.0522 | 650 | 19.0120 |
| 75 | 0.0690 | 275 | 5.1561 | 475 | 12.9935 | 675 | 19.7904 |
| 100 | 0.2541 | 300 | 6.1357 | 500 | 13.9153 | 700 | 20.5498 |
| 125 | 0.5915 | 325 | 7.1308 | 525 | 14.8167 | 725 | 21.2906 |
| 150 | 1.0835 | 350 | 8.1310 | 550 | 15.6972 | 750 | 22.0135 |
| 175 | 1.7150 | 375 | 9.1284 | 575 | 16.5568 | 775 | 22.7191 |
| 200 | 2.4626 | 400 | 10.117 | 600 | 17.3956 | 800 | 23.4080 |

8. Zn

| T [K] | S [J/K/mol] | T [K] | S [J/K/mol] | T [K] | S [J/K/mol] | T [K] | S [J/K/mol] |
|---------|---------------|---------|---------------|---------|---------------|---------|---------------|
| 25 | 4.7968 | 225 | 42.0395 | 425 | 57.3580 | 625 | 66.7984 |
| 50 | 12.0016 | 250 | 44.5407 | 450 | 58.7529 | 650 | 67.7615 |
| 75 | 18.4567 | 275 | 46.8192 | 475 | 60.0739 | 675 | 68.6886 |
| 100 | 23.9634 | 300 | 48.9104 | 500 | 61.3285 | 700 | 69.5823 |
| 125 | 28.6435 | 325 | 50.8420 | 525 | 62.5229 | 725 | 70.4450 |
| 150 | 32.6659 | 350 | 52.6362 | 550 | 63.6627 | 750 | 71.2786 |
| 175 | 36.1722 | 375 | 54.3109 | 575 | 64.7525 | 775 | 72.0851 |
| 200 | 39.2701 | 400 | 55.8807 | 600 | 65.7965 | 800 | 72.8662 |

* thonhauser@wfu.edu

- ¹ J. Graetz, Chem. Soc. Rev. **38**, 73 (2009).
- ² E. Rönnebro, Curr. Opin. Solid State Mater. Sci. **15**, 44 (2011).
- ³ H.-W. Li, Y. Yan, S.-i. Orimo, A. Züttel, and C. M. Jensen, Energies **4**, 185 (2011).
- ⁴ L. H. Rude, T. K. Nielsen, D. B. Ravnsbaek, U. Bösenberg, M. B. Ley, B. Richter, L. M. Arnbjerg, M. Dornheim, Y. Filinchuk, F. Besenbacher, and T. R. Jensen, Phys. Status Solidi A **208**, 1754 (2011).
- ⁵ I. P. Jain, P. Jain, and A. Jain, J. Alloys Compd. **503**, 303 (2010).
- ⁶ DOE Targets for Onboard Hydrogen Storage Systems for Light-Duty Vehicles, retrieved from http://energy.gov/sites/prod/files/2014/03/f12/targets_onboard_hydro_storage.pdf (US Department of Energy, 2009) – for a good side-by-side comparison between the old and new DOE targets see Ref. [7].
- ⁷ J. Yang, A. Sudik, C. Wolverton, and D. J. Siegel, Chem. Soc. Rev. **39**, 656 (2010).
- ⁸ J. J. Vajo, S. L. Skeith, and F. Mertens, J. Phys. Chem. B **109**, 3719 (2005).
- ⁹ S. V. Alapati, K. J. Johnson, and D. S. Sholl, Phys. Chem. Chem. Phys. **9**, 1438 (2007).
- ¹⁰ S. V. Alapati, J. K. Johnson, and D. S. Sholl, J. Phys. Chem. C **112**, 5258 (2008).
- ¹¹ H.-W. Li, K. Kikuchi, Y. Nakamori, N. Ohba, K. Miwa, S. Towata, and S. Orimo, Acta Mater. **56**, 1342 (2008).
- ¹² E. A. Nickels, M. O. Jones, W. I. F. David, S. R. Johnson, R. L. Lowton, M. Sommariva, and P. P. Edwards, Angew. Chemie Int. Ed. **47**, 2817 (2008).
- ¹³ K. Hoang and C. G. Van de Walle, Phys. Rev. B **80**, 214109 (2009).
- ¹⁴ M. J. van Setten, G. A. de Wijs, and G. Brocks, Phys. Rev. B **76**, 075125 (2007).
- ¹⁵ H. W. Brinks, A. Fossdal, and B. C. Hauback, J. Phys. Chem. C **112**, 5658 (2008).
- ¹⁶ H.-W. Li, K. Kikuchi, Y. Nakamori, K. Miwa, S. Towata, and S. Orimo, Scr. Mater. **57**, 679 (2007).
- ¹⁷ G. Severa, E. Rönnebro, and C. M. Jensen, Chem. Commun. **46**, 421 (2010).
- ¹⁸ G. L. Soloveichik, Y. Gao, J. Rijssenbeek, M. Andrus, S. Kniajanski, R. C. Bowman, Jr., S.-J. Hwang, and J.-C. Zhao, Int. J. Hydrogen Energy **34**, 916 (2009).
- ¹⁹ V. Ozoliņš, E. H. Majzoub, and C. Wolverton, Phys. Rev. Lett. **100**, 135501 (2008).
- ²⁰ E. Albanese, G. N. Kalantzopoulos, J. G. Vitillo, E. Pina-tel, B. Civalleri, S. Deledda, S. Bordiga, B. C. Hauback, and M. Baricco, J. Alloys Compd. **580**, S282 (2013).
- ²¹ Y. Zhang, E. Majzoub, V. Ozoliņš, and C. Wolverton, J. Phys. Chem. C **116**, 10522 (2012).
- ²² M. J. van Setten, G. A. de Wijs, M. Fichtner, and G. Brocks, Chem. Mater. **20**, 4952 (2008).
- ²³ T. D. Huan, M. Amsler, R. Sabatini, V. N. Tuoc, N. B. Le, L. M. Woods, N. Marzari, and S. Goedecker, Phys. Rev. B **88**, 024108 (2013).
- ²⁴ A. Bil, B. Kolb, R. Atkinson, D. G. Pettifor, T. Thonhauser, and A. N. Kolmogorov, Phys. Rev. B **83**, 224103 (2011).
- ²⁵ Y. Nakamori, K. Miwa, A. Ninomiya, H. Li, N. Ohba, S. I. Towata, A. Züttel, and S. I. Orimo, Phys. Rev. B **74**, 045126 (2006).

- ²⁶ Using the entire experimental data from Ref. 27 on all borohydrides yields a fit of $T_d = 1435 - 675.0\chi_P$ and $T_d = 439.4 + 6.71\Delta H_f$. The fits here were obtained by limiting the experimental data to all borohydrides with double-valence metals.
- ²⁷ Y. Nakamori, H.-W. Li, K. Kikuchi, M. Aoki, K. Miwa, S. Towata, and S. Orimo, *J. Alloys Compd.* **446-447**, 296 (2007).
- ²⁸ E. Jeon and Y. Cho, *J. Alloys Compd.* **422**, 273 (2006).
- ²⁹ G. N. Kalantzopoulos, J. G. Vitillo, E. Albanese, E. Pinatell, B. Civalieri, S. Deledda, S. Bordiga, M. Baricco, and B. C. Hauback, *J. Alloys Compd.* , 10 (2014), in press.
- ³⁰ D. Ravnsbaek, Y. Filinchuk, Y. Cerenius, H. J. Jakobsen, F. Besenbacher, J. Skibsted, and T. R. Jensen, *Angew. Chemie Int. Ed.* **48**, 6659 (2009).
- ³¹ K. Miwa, N. Ohba, S. Towata, Y. Nakamori, and S. Orimo, *J. Alloys Compd.* **404-406**, 140 (2005).
- ³² G. Kresse and J. Furthmüller, *Phys. Rev. B* **54**, 11169 (1996).
- ³³ G. Kresse and D. Joubert, *Phys. Rev. B* **59**, 1758 (1999).
- ³⁴ M. J. van Setten, M. A. Uijttewaai, G. A. de Wijs, and R. A. de Groot, *J. Am. Chem. Soc.* **129**, 2458 (2007).
- ³⁵ Z. Lodziana, *Phys. Rev. B* **81**, 144108 (2010).
- ³⁶ T. Thonhauser, V. R. Cooper, S. Li, A. Puzder, P. Hyldgaard, and D. C. Langreth, *Phys. Rev. B* **76**, 125112 (2007).
- ³⁷ D. C. Langreth, B. I. Lundqvist, S. D. Chakarova-Käck, V. R. Cooper, M. Dion, P. Hyldgaard, A. Kelkkanen, J. Kleis, L. Kong, S. Li, P. G. Moses, E. D. Murray, A. Puzder, H. Rydberg, E. Schröder, and T. Thonhauser, *J. Phys. Condens. Matter* **21**, 084203 (2009).
- ³⁸ M. Dion, H. Rydberg, E. Schröder, D. C. Langreth, and B. I. Lundqvist, *Phys. Rev. Lett.* **92**, 246401 (2004).
- ³⁹ G. Henkelman, A. Arnaldsson, and H. Jónsson, *Comput. Mat. Sci.* **36**, 254 (2006).
- ⁴⁰ H. Hemmes, A. Driessen, and R. Griessen, *J. Phys. C* **19**, 3571 (1986).
- ⁴¹ Y. Yan, H.-W. Li, Y. Nakamori, N. Ohba, K. Miwa, S.-i. Towata, and S.-i. Orimo, *Mater. Trans.* **49**, 2751 (2008).
- ⁴² J. J. Vajo, F. Mertens, C. C. Ahn, R. C. Bowman, and B. Fultz, *J. Phys. Chem. B* **108**, 13977 (2004).
- ⁴³ G. Balducci, S. Brutti, A. Ciccioli, G. Gigli, P. Manfrinetti, A. Palenzona, M. F. Butman, and L. Kudin, *J. Phys. Chem. Solids* **66**, 292 (2005).
- ⁴⁴ The authors of Ref. [41] propose here the decomposition of $\text{MgB}_{12}\text{H}_{12}$ before MgH_2 , which we find to be unlikely as it has a critical temperature of 716 K. We suspect the actual reaction studied was the one we proposed.
- ⁴⁵ V. Ozoliņš, E. H. Majzoub, and C. Wolverton, *J. Am. Chem. Soc.* **131**, 230 (2009).
- ⁴⁶ R. J. Newhouse, V. Stavila, S.-J. Hwang, L. E. Klebanoff, and J. Z. Zhang, *J. Phys. Chem. C* **114**, 5224 (2010).
- ⁴⁷ Y. Yan, H.-W. Li, H. Maekawa, M. Aoki, T. Noritake, M. Matsumoto, K. Miwa, S.-i. Towata, and S.-i. Orimo, *Mater. Trans.* **52**, 1443 (2011).
- ⁴⁸ J. Yang, X. Zhang, J. Zheng, P. Song, and X. Li, *Scripta Mater.* **64**, 225 (2011).
- ⁴⁹ Y. Zhang, E. Majzoub, V. Ozoliņš, and C. Wolverton, *Phys. Rev. B* **82**, 174107 (2010).
- ⁵⁰ T. Matsunaga, F. Buchter, P. Mauron, M. Bielman, Y. Nakamori, S. Orimo, N. Ohba, K. Miwa, S. Towata, and A. Züttel, *J. Alloys Compd.* **459**, 583 (2008).
- ⁵¹ A. Züttel, P. Wenger, S. Rentsch, P. Sudan, P. Mauron, and C. Emmenegger, *J. Power Sources* **118**, 1 (2003).